Image Segmentation for Reflected-Light Microscopy: Some Theoretical Approaches

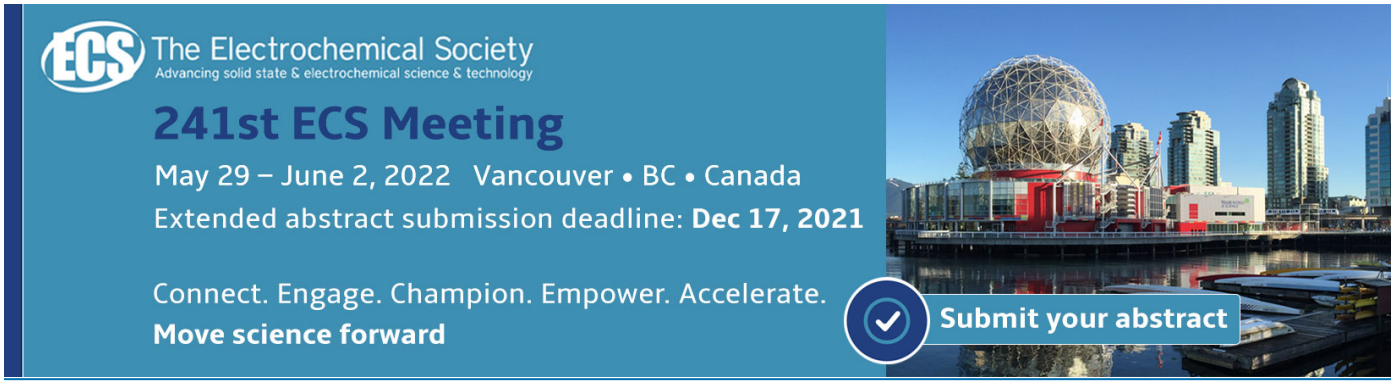

Image Segmentation for Reflected-Light Microscopy: Some Theoretical Approaches

Stefano Pagnotta[1], Andrea Aquino [1], Marco Lezzerini [1]

[1] Earth Science Department - University of Pisa, Via S. Maria 53, 56126 Pisa, Italy

stefano.pagnotta@unipi.it

Abstract. Often when we approach the study of lithologies coming from the urban environment, but in general, even from any other environment, be it a quarry, a mine, an outcrop of our interest, the first study we carry out is the one in reflected-light optical-microscopy. Reflected-light microscopy in respect to transmitted-light microscopy requires minimal sample preparation, having to polish a single surface and without the need to thin the samples to allow light to pass through them. It may be useful, already in the first analysis, to try to produce quantitative data on what we are observing. A further advantage of reflected light in an urban environment is that of being able to observe and describe the formation or interaction between opaque minerals and the environment. Information that we lose by passing directly to the transmitted light. The information that can be useful to us and that we can obtain are the relative porosity of the sample, the texture (when easily recognizable in reflected light), the maximum size and shape of the edges of the grains. To all this is added the relationship between the areas of the different crystallites identified and the possible background mass, which cannot be solved on the observation scale. When we are dealing with many samples, we do not always have the time to be able to study individually sample by sample through images, so we resort to the use of image analysis tools for image segmentation and analysis. Among these, the main thresholding method with the Otsu method, the segmentation with the k averages algorithm, and, finally, a neural network of the SOM type. In this short work, we will review the main methods of image segmentation plus an innovative method developed by our group, highlighting its strengths and weaknesses.

1. Introduction

In Tuscany, walking through places inhabited by the Etruscans, everyone will have come across small pebbles or fragments of dark materials with a metallic sheen. They probably are hematite, coming from the Island of Elba, which has now become part of the context of ancient urban geology [1]. Following the Punic wars, this mineral, coming from the Island of Elba (Tuscan Archipelago, Italy) became the main source for obtaining the iron useful for producing the swords used by the ancient Romans [2,3]. The production of this metal has generated in the area of the Gulf of Baratti (Tuscany, Italy) a considerable accumulation of raw mineral in the form of minute fragments of rock, sand and fine dust, as well as an abundant presence of melting slag [2].The common first analytical approach towards these materials is constituted by optical microscopy (OM) as suggested by several authors [4–6] and only after by XRF, XRD, SEM and XANES [7]. At the current state of research, a new method based on the analysis of rare earth elements (REE) carried out on the sediments in place could lead to an identification of the FeOx layers formed by natural processes, distinguishing them from the actually anthropogenic ones [8]. In the field of geomaterials analysis, when we refer to OM, we immediately think about

transmitted light. The possibility of working also in reflected light offers us at least two advantages: i) by simply polishing one face of the sample we can obtain useful information; ii) we can also obtain information on those minerals that instead reflect light (opaque) which also have their importance in understanding the type of material, its texture, and the relationships between the different crystallites present. When we take samples of a geomaterial, coming from the urban environment, having to prepare it for analysis in transmitted light, it would always be useful to analyse a polished face also in reflected light. The Vickers micro-hardness together with the micro-spectrophotometry (MSP), remains today the preferred aid in the identification of opaque minerals in specimens for reflected light microscopy [9]. With the development of new technologies and the increasingly important presence in the research of analysis algorithms, classification and segmentation techniques have become increasingly routine. In some sectors such as diagnostics applied to cultural heritage [10–16], segmentation techniques, sometimes even very advanced ones, are on the agenda [17–21]. In the field of geomaterials, there are several applications of image segmentation analysis, especially as regards the identification, classification, and quantification of iron ore [4,5,22–25]. The use of neural networks for the segmentation of images in the analysis of geomaterials has been addressed in several works concerning elementary mapping using LIBS spectroscopy [26–29], where it has proved to be very effective and functional in obtaining segments with the same properties of element associations, for fast clustering and analysis using calibration-free methods (CF). The image segmentation carried out by optical microscopy in reflected light is very complex [30]. There are several factors in the capture of microscope images that can create noise in the acquired image. An image carried out by reflected microscopy is composed mainly of a Light signal plus a noise as follows:

$$I=S_I+N \tag{1}$$

where I is the acquired image, S_I is the light reflected from the sample and N is the mixed noise. The noise N is the sum of different types of noise: electronic noise, due to the high sensitivity of the CCD sensor used, white noise due to the white balancing of the image, and instrumental noise due to the optical path of the microscope. To reduce the influence of this noise on the acquired image, we can calibrate our image by acquiring in the same conditions of acquisition of the sample image also a dark image (a photograph taken with the camera shutter completely closed) and an image of the white (a photo taken on a white reference) [31–36]. The subtraction of dark reference reduces the effect of electronic noise due to the high sensitivity of the CCD, while the subtraction of white balances the white of the image and reduces the effects of chromatic aberration due to the optical path of the microscope [37]. Before starting to work with any type of image it is good to carry out a calibration of the same using the black and white references, with the following formula:

$$I_{corr} = \frac{(I_{x,y}-Bl_{x,y})}{(Wh_{x,y}-Bl_{x,y})}\ N \tag{2}$$

where I_{corr} is the corrected image, $I_{x,y}$ correspond to each pixel of uncorrected image I, $Bl_{x,y}$ correspond to each pixel of the dark image (for evaluation of the electrical noise) and $Wh_{x,y}$ correspond to each pixel in the image taken on a white reference.
This work aims to briefly illustrate some methods for segmentation of images obtained under the microscope in reflected light, showing the results and putting light on its strengths and weaknesses. A short Live Script made in MATLAB was used to carry out the analysis.

2. Material and methods

For this work, we decided to use a hematite sample (Figure 1) that we have embedded in a red-colored epoxy resin and polished on the upper surface to highlight the crystals structures, the resin pores present, and to be able to carry out the image segmentation. We have chosen to work on this mineral because it has a simple structure on which to show how the different segmentation algorithms work. Furthermore,

we have deliberately allowed residues of polishing dust to accumulate in the pores, to show the robustness of some methods in being able to separate this material. The image was acquired using an industrial reflected light microscope equipped with a 14-megapixel CCD camera. To speed up the analysis, the program that has been written in MATLAB allows you to select an ROI on which to carry out the segmentation, reducing the number of pixels to be analyzed and speed up the elaboration time.

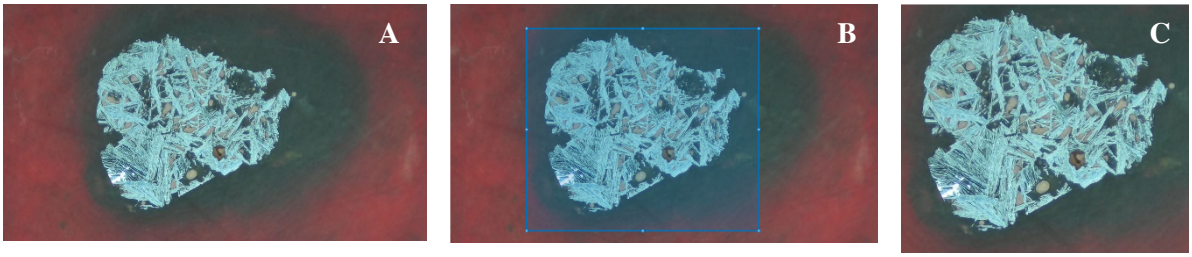

Figure 1. Hematite sample. A) Total sample image, the image represents an area of 20 x 11.25 mm^2; B) position of the selected ROI area; C) ROI image, the image represents an ROI of 10.8 x 9.4mm^2.

After selecting the ROI that interests us on the photographed area of the sample under analysis, we can proceed with different segmentation methods.

2.1. Otsu thresholding

Certainly, when an image must be segmented, the first method that comes to mind is that of Otsu thresholding [38–40]. In few words, the algorithm allows us, once our colour image has been transformed into grayscale, to find a unique grey-value (global threshold value T) for which the pixels are divided into two classes: foreground and background. The T value was used to binarize the grayscale image as follow:

$$p_{bin}=0 \text{ if } p_{gray}<T \; N \quad (3)$$

$$p_{bin}=1 \text{ if } p_{gray}>T \; N \quad (4)$$

Where p_{bin} is the pixel value in the new binarized image and p_{gray} is the original grayscale image pixel value. This method is relatively simple to implement and is very effective in less complex images with few details.

2.2. Triangle method thresholding

If there are very weak peaks in the histogram, due to small details of the image, such as, in our case, blistering due to the resin, the triangle method can be very useful.
A line is constructed between the maximum of the histogram at (b) and the lowest (or highest depending on context) value (a) in the histogram. The distance L normal to the line and between the line and the histogram h(b) is computed for all values from a to b. The level where the distance between the histogram and the line is maximal is the threshold value (level). This technique is particularly effective when the object pixels produce a weak peak in the histogram [41].

2.3. K-means segmentation

The k-means method consists of the subdivision of n observations into k clusters to which all the observations with the mean closest to the centre (or centroid) of the cluster will belong. The result of this algorithm leads to a partitioning of the space in what are the Voronoi [42] cells, based on the method of calculating the distance of each observation from the centroid of the cluster, different results can be obtained [43].

2.4. Self-Organized Maps segmentation

Self-organizing maps belong to the series of artificial intelligence algorithms, which involve unsupervised training to produce a reduction in feature space. This means that given a set of images I^n in which different features of the sample under analysis are reproduced, where n represents the space of the features, during the training of the SOM this space will be reduced to a size equal to the number of neurons chosen for the network. The result obtained is a new set of binary images (where 0 = black and 1 = white), which represent a dimensional reduction of the space of the incoming features. The results of this dimensional scaling can be very interesting for the segmentation of images as they tend to combine those features that have a correlation between them that is not simply spatial but also concerns the behaviour of reflected light [44–47].

3. Results and discussions

The first type of segmentation we applied, based on a grey threshold using the Otsu algorithm returns the image in the Figure 2 on the left. We can observe how it is possible to simply separate the embedding resin from what is the mineral sample, while the polishing dust, deposited in the pores, is segmented together with the mineral. As previously written, this method is very powerful in the case of very simple images that have very distinct areas consisting of only two components. As can be seen from the image, the area occupied by the hematite is well segmented although the porous areas filled with polishing residues also fall into the same segment.

The triangle thresholding method is very efficient if we are faced with an image that has very low peaks in the histogram (Figure 2 on the right).

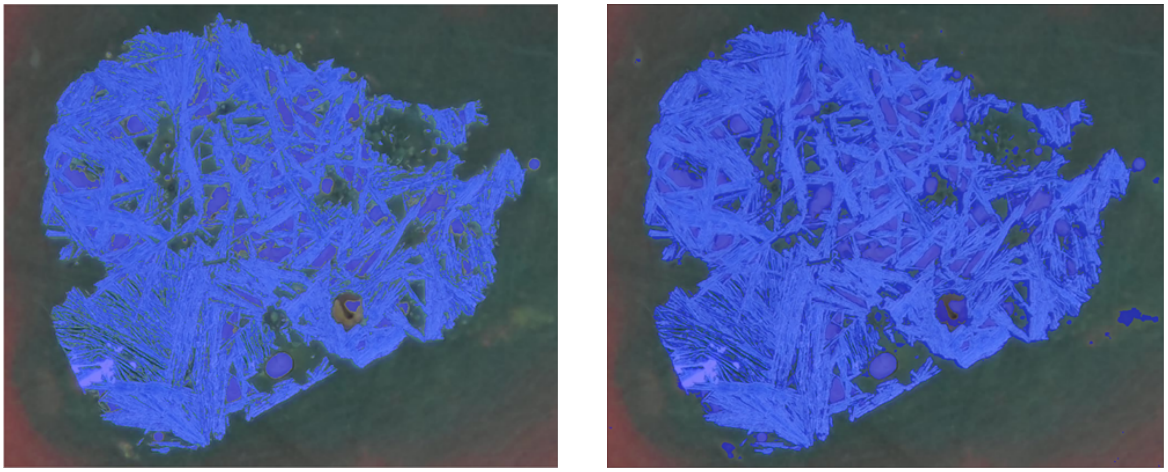

Figure 2. Segmentation with Otsu grey threshold on the left and triangle method on the right.

The interesting feature of this method is to be able to threshold elements that have low-intensity peaks within the histogram (Figure 3). In this case, we can see how the triangle method has also managed to segment the mineral that can be glimpsed below the embedding resin and at the same time presents a much clearer border demarcation. Reading the histogram of the image with indicated the threshold points for both methods allows us to understand the reason for this different segmentation: while the threshold value for the Otsu method is centered on the maximum of the histogram, the threshold value for the triangle method was centered on the first of the two large and low peaks present, consisting of values shifted more towards white and with a wider distribution (Figure 3).

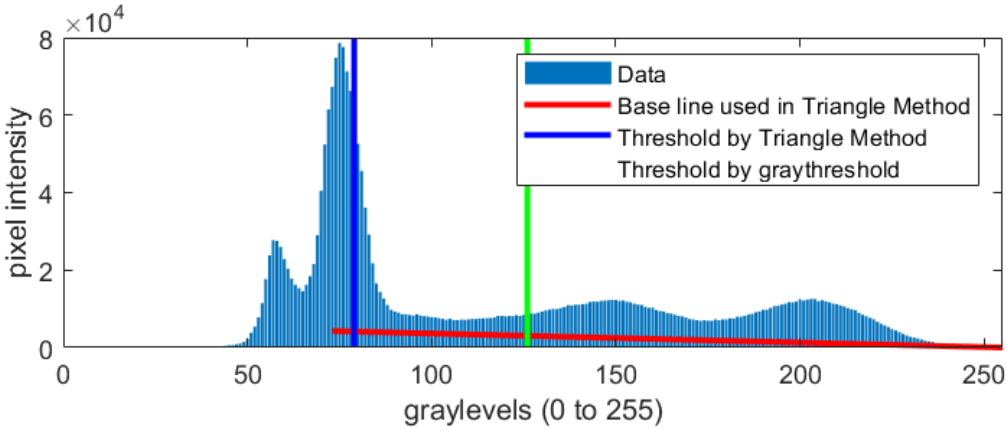

Figure 3. Gray levels Histogram of the ROI. The green peak line identifies the threshold value obtained with the triangle method while the blue peak line identifies the threshold value for the Otsu method.

The segmentation with the method of k-means comes to our aid when in the histogram of our ROI, there are several peaks (as in our case). The k-means can be chosen on a heuristic basis, or the value of k can be chosen automatically, based on the number of peaks identified in the ROI histogram (as in our case).

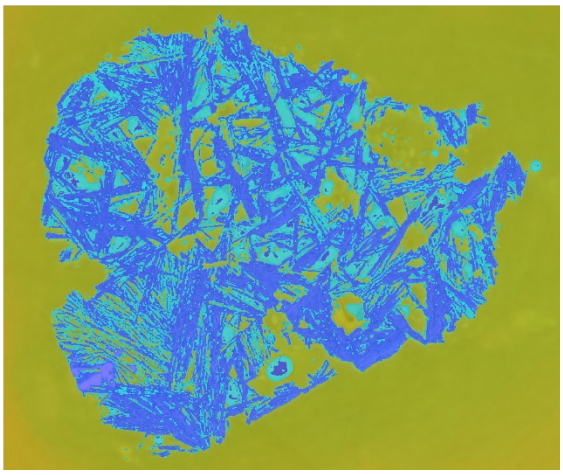

Figure 4. The K-means segmentation results.

Four distinct peaks are identified in the histogram (Figure 3), two very narrow and intense peaks in the portion referable to dark grey tones and two very wide and not very intense peaks in the portion attributable to light grey tones. This leads to a segmentation of the image into four distinct features corresponding to the mineral, the polishing dust deposited in the pores, the resin, and the edges of the pores. This segment is due to the variation in light intensity of the mineral in contact with the pores and with the resin. It is noted that although the segments reflect the actual characteristics of the ROI investigated, their limits are not yet well defined and precise.

For some time our research group has been using self-organized maps (SOM) to segment elementary maps made with a scanning micro-LIBS system [26,29,48]. Having already proven its effectiveness in the segmentation of images that present minor problems compared to those made using an optical reflected light microscope, we decided to try to apply the method also in this area.

SOM-type neural networks can segment images based on the characteristics generated by the physical properties of the material and at the same time preserve their topology. This has the consequence of generating a precise segmentation from the point of view of the recognized features, but

also of the precision of their limits. However, it must be borne in mind that everything depends on optimizing the choice of the number of neurons in the network. The optimization is carried out in this short study by performing several experiments with an increasing number of neurons. Since, it has been noticed that already with five neurons some features that belong to the same object are separated, we have opted for four neurons.

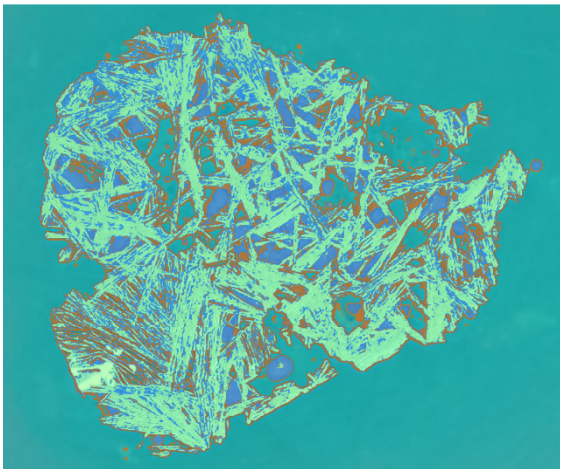

Figure 5. SOM segmentation of ROI. Cian and Blue represent the Resin and the polishing residues, light green represent the mineral, and brown the limit of ore mineral.

If we look at the individual segments of the ROI, we can more easily identify the texture of the mineral and the respective percentage areas occupied by the segmented features.

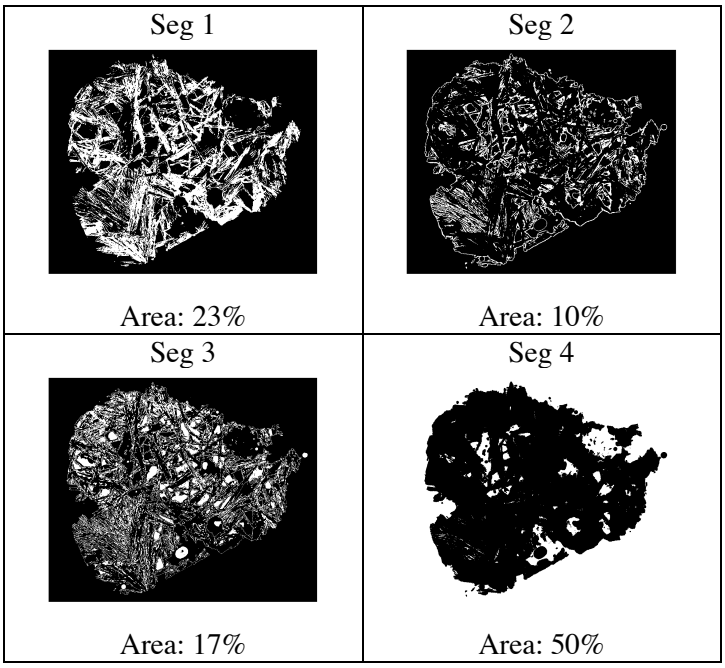

Figure 6. Results of the individual segments of the ROI with relative pixel area (%).

4. Conclusions

In the segmentation of the image in reflected-light microscopy, there are several factors to be considered, which can constitute a problem in the segmentation and interpretation of the images. To mitigate some of these problems there are simple algorithms that allow obtaining good starting images. The classical thresholding methods are very effective in the case of non-complex images. Where the elements to be

separated are few and already well defined and contrasted. The segmentation is carried out with the k-means method, where the parameter k is automatically chosen on the histogram of the image, it is possible to obtain a better separation and definition of the different areas of the observed sample. The SOM neural network requires a careful choice of the number of neurons on a heuristic basis. Being guided by the knowledge of the operator allows a better clustering of the sample, while providing natively binarized images (the SOM clusters), on which it is possible to directly perform area calculations. The criteria on which we based our evaluation of image quality, following the indications of Haralick & Shapiro [49] are based on an evaluation of the characteristic criteria and of the semantic criteria. Based on these parameters, the segmentation obtained through the neural network is the best among the algorithms proposed in this short work.

References

[1] L. Chiarantini, M. Benvenuti, P. Costagliola, M.E. Fedi, S. Guideri, A. Romualdi, Copper production at Baratti (Populonia, southern Tuscany) in the early Etruscan period (9th–8th centuries BC), J. Archaeol. Sci. 36 (2009) 1626–1636.
[2] P. Crew, The iron and copper slags at Baratti, Populonia, Italy, Hist. Metall. Hist. Metall. Soc. 25 (1991) 109–115.
[3] A. Cartocci, M.E. Fedi, F. Taccetti, M. Benvenuti, L. Chiarantini, S. Guideri, Study of a metallurgical site in Tuscany (Italy) by radiocarbon dating, Nucl. Instruments Methods Phys. Res. Sect. B Beam Interact. with Mater. Atoms. 259 (2007) 384–387.
[4] O. da F.M. Gomes, J.C.A. Iglesias, S. Paciornik, M.B. Vieira, Classification of hematite types in iron ores through circularly polarized light microscopy and image analysis, Miner. Eng. 52 (2013) 191–197.
[5] O.D.M. Gomes, S. Paciornik, Iron ore quantitative characterisation through reflected light-scanning electron co-site microscopy, in: Int. Congr. Appl. Mineral., 2008: pp. 699–702.
[6] E. Donskoi, S. Hapugoda, J.R. Manuel, A. Poliakov, M.J. Peterson, H. Mali, B. Bückner, T. Honeyands, M.I. Pownceby, Automated Optical Image Analysis of Iron Ore Sinter, Minerals. 11 (2021) 562.
[7] R. Hiraga, O. da F.M. Gomes, R. Neumann, Maghemite in Brazilian Iron Ores: Quantification of the Magnetite-Maghemite Isomorphic Series by X-ray Diffraction and the Rietveld Method, and Confirmation by Independent Methods, Minerals. 11 (2021) 346.
[8] G. Gallello, J. Bernabeu, A. Díez Castillo, P. Escribá Ruiz, A. Pastor, M. Lezzerini, S. Chenery, M.E. Hodson, D. Stump, Developing REE parameters for soil and sediment profile analysis to identify Neolithic anthropogenic signatures at Serpis Valley (Spain), Atti Della Soc. Toscana Di Sci. Nat. Mem. Ser. A, 2020, Vol. 126, p. 13-32. (2020).
[9] P. Ramdohr, The ore minerals and their intergrowths, Elsevier, 2013.
[10] E.M. Payne, Imaging techniques in conservation, J. Conserv. Museum Stud. 10 (2013).
[11] G. Filippidis, G.J. Tserevelakis, A. Selimis, C. Fotakis, Nonlinear imaging techniques as non-destructive, high-resolution diagnostic tools for cultural heritage studies, Appl. Phys. A. 118 (2015) 417–423.
[12] M. Picollo, C. Cucci, A. Casini, L. Stefani, Hyper-spectral imaging technique in the cultural heritage field: new possible scenarios, Sensors. 20 (2020) 2843.
[13] F. Stanco, S. Battiato, G. Gallo, Digital imaging for cultural heritage preservation: Analysis, restoration, and reconstruction of ancient artworks, CRC Press, 2017.
[14] E. Marengo, M. Manfredi, O. Zerbinati, E. Robotti, E. Mazzucco, F. Gosetti, G. Bearman, F. France, P. Shor, Development of a technique based on multi-spectral imaging for monitoring the conservation of cultural heritage objects, Anal. Chim. Acta. 706 (2011) 229–237.
[15] S. George, J.Y. Hardeberg, J. Linhares, L. Macdonald, C. Montagner, S. Nascimento, M. Picollo, R. Pillay, T. Vitorino, E.K. Webb, A study of spectral imaging acquisition and processing for cultural heritage, in: Digit. Tech. Doc. Preserv. Cult. Herit., ARC, Amsterdam University Press, 2018: pp. 141–158.

[16] E. Peccenini, F. Albertin, M. Bettuzzi, R. Brancaccio, F. Casali, M.P. Morigi, F. Petrucci, Advanced imaging systems for diagnostic investigations applied to Cultural Heritage, in: J. Phys. Conf. Ser., IOP Publishing, 2014: p. 12022.
[17] G. Sansoni, M. Trebeschi, F. Docchio, State-of-the-art and applications of 3D imaging sensors in industry, cultural heritage, medicine, and criminal investigation, Sensors. 9 (2009) 568–601.
[18] D. Mannes, E. Lehmann, A. Masalles, K. Schmidt-Ott, K. Schaeppi, F. Schmid, S. Peetermans, K. Hunger, The study of cultural heritage relevant objects by means of neutron imaging techniques, Insight-Non-Destructive Test. Cond. Monit. 56 (2014) 137–141.
[19] C. Andreani, G. Gorini, T. Materna, Novel neutron imaging techniques for cultural heritage objects, in: Neutron Imaging Appl., Springer, 2009: pp. 229–252.
[20] M. Hess, S. Robson, 3D colour imaging for cultural heritage artefacts, Int. Arch. Photogramm. Remote Sens. Spat. Inf. Sci. 38 (2010) 288–292.
[21] M.M. Morita, G.M. Bilmes, Applications of low-cost 3D imaging techniques for the documentation of heritage objects, (2018).
[22] F. Nellros, M.J. Thurley, Automated image analysis of iron-ore pellet structure using optical microscopy, Miner. Eng. 24 (2011) 1525–1531.
[23] O.D.M. Gomes, S. Paciornik, J.C.A. Iglesias, A simple methodology for identifying hematite grains under polarized reflected light microscopy, in: Proc. 17th Int. Conf. Syst. Signals Image Process., 2010: pp. 428–431.
[24] J.C.Á. Iglesias, K.S. Augusto, O. da F.M. Gomes, A.L.A. Domingues, M.B. Vieira, C. Casagrande, S. Paciornik, Automatic characterization of iron ore by digital microscopy and image analysis, J. Mater. Res. Technol. 7 (2018) 376–380.
[25] J.C.A. Iglesias, O. da F.M. Gomes, S. Paciornik, Automatic recognition of hematite grains under polarized reflected light microscopy through image analysis, Miner. Eng. 24 (2011) 1264–1270.
[26] S. Živković, A. Botto, B. Campanella, M. Lezzerini, M. Momčilović, S. Pagnotta, V. Palleschi, F. Poggialini, S. Legnaioli, Laser-Induced Breakdown Spectroscopy elemental mapping of the construction material from the Smederevo Fortress (Republic of Serbia), Spectrochim. Acta Part B At. Spectrosc. (2021) 106219.
[27] S. Pagnotta, S. Legnaioli, B. Campanella, E. Grifoni, M. Lezzerini, G. Lorenzetti, V. Palleschi, F. Poggialini, S. Raneri, Micro-chemical evaluation of ancient potsherds by μ-LIBS scanning on thin section negatives, Mediterr. Archaeol. Archaeom. 18 (2018) 171–178. https://doi.org/10.5281/zenodo.1285906.
[28] S. Pagnotta, M. Lezzerini, B. Campanella, G. Gallello, E. Grifoni, S. Legnaioli, G. Lorenzetti, F. Poggialini, S. Raneri, A. Safi, V. Palleschi, Fast quantitative elemental mapping of highly inhomogeneous materials by micro-Laser-Induced Breakdown Spectroscopy, Spectrochim. Acta - Part B At. Spectrosc. 146 (2018). https://doi.org/10.1016/j.sab.2018.04.018.
[29] G.S. Senesi, B. Campanella, E. Grifoni, S. Legnaioli, G. Lorenzetti, S. Pagnotta, F. Poggialini, V. Palleschi, O. De Pascale, Elemental and mineralogical imaging of a weathered limestone rock by double-pulse micro-Laser-Induced Breakdown Spectroscopy, Spectrochim. Acta - Part B At. Spectrosc. 143 (2018). https://doi.org/10.1016/j.sab.2018.02.018.
[30] N. Ramou, N. Chetih, Y. Boutiche, R. Abdelkader, Automatic image segmentation for material microstructure characterization by optical microscopy, Informatica. 44 (2020).
[31] N. Teranishi, N. Mutoh, Partition noise in CCD signal detection, IEEE Trans. Electron Devices. 33 (1986) 1696–1701.
[32] N.J. Hangiandreou, T.J. O'Connor, J.P. Felmlee, An evaluation of the signal and noise characteristics of four CCD-based film digitizers, Med. Phys. 25 (1998) 2020–2026.
[33] J.-M. Woo, H.-H. Park, S.-M. Hong, I.-Y. Chung, H.S. Min, Y.J. Park, Statistical noise analysis of CMOS image sensors in dark condition, IEEE Trans. Electron Devices. 56 (2009) 2481–2488.
[34] G.R. Hopkinson, D.H. Lumb, Noise reduction techniques for CCD image sensors, J. Phys. E. 15 (1982) 1214.
[35] M. Bigas, E. Cabruja, J. Forest, J. Salvi, Review of CMOS image sensors, Microelectronics J.

37 (2006) 433–451.
[36] X. Zhen, Elimination of image noise with CCD device characteristics, Opto-Electronic Eng. (2001) 6.
[37] E. Pirard, Multispectral imaging of ore minerals in optical microscopy, Mineral. Mag. 68 (2004) 323–333.
[38] N. Otsu, A threshold selection method from gray-level histograms, IEEE Trans. Syst. Man. Cybern. 9 (1979) 62–66.
[39] X. Xu, S. Xu, L. Jin, E. Song, Characteristic analysis of Otsu threshold and its applications, Pattern Recognit. Lett. 32 (2011) 956–961.
[40] L. Jianzhuang, L. Wenqing, T. Yupeng, Automatic thresholding of gray-level pictures using two-dimension Otsu method, in: China., 1991 Int. Conf. Circuits Syst., IEEE, 1991: pp. 325–327.
[41] G.W. Zack, W.E. Rogers, S.A. Latt, Automatic measurement of sister chromatid exchange frequency., J. Histochem. Cytochem. 25 (1977) 741–753.
[42] M. Erwig, The graph Voronoi diagram with applications, Networks An Int. J. 36 (2000) 156–163.
[43] N. Dhanachandra, K. Manglem, Y.J. Chanu, Image segmentation using K-means clustering algorithm and subtractive clustering algorithm, Procedia Comput. Sci. 54 (2015) 764–771.
[44] N. Senthilkumaran, R. Rajesh, Image segmentation-a survey of soft computing approaches, in: 2009 Int. Conf. Adv. Recent Technol. Commun. Comput., IEEE, 2009: pp. 844–846.
[45] A. Wismüller, F. Vietze, J. Behrends, A. Meyer-Baese, M. Reiser, H. Ritter, Fully automated biomedical image segmentation by self-organized model adaptation, Neural Networks. 17 (2004) 1327–1344.
[46] M. V Akinin, A.I. Taganov, M.B. Nikiforov, A. V Sokolova, Image segmentation algorithm based on self-organized Kohonen's neural maps and tree pyramidal segmenter, in: 2015 4th Mediterr. Conf. Embed. Comput., IEEE, 2015: pp. 168–170.
[47] H. Hoffmann, D.W. Payton, Optimization by self-organized criticality, Sci. Rep. 8 (2018) 1–9.
[48] A. Botto, B. Campanella, S. Legnaioli, M. Lezzerini, G. Lorenzetti, S. Pagnotta, F. Poggialini, V. Palleschi, Applications of laser-induced breakdown spectroscopy in cultural heritage and archaeology: a critical review, J. Anal. At. Spectrom. 34 (2019) 81–103.
[49] R.M. Haralick, L.G. Shapiro, Image segmentation techniques, Comput. Vision, Graph. Image Process. 29 (1985) 100–132.